

# Low-frequency turbulent transport in magnetron plasmas

T. E. Sheridan and J. Goree

*Department of Physics and Astronomy, The University of Iowa, Iowa City, Iowa 52242-1410*

(Received 19 August 1988; accepted 10 October 1988)

We report the results of an experiment to determine if low-frequency turbulence (frequencies less than the ion plasma frequency) seen in magnetron plasmas is responsible for the transport of electrons across magnetic field lines. This is done by finding the scaling of the electron confinement time  $\tau$  on the mean-square electric field fluctuation  $\langle |\delta E|^2 \rangle$ . Turbulent transport models predict the scaling should be  $\tau \propto \langle |\delta E|^2 \rangle^{-1}$ . Data were taken at a constant pressure of 1.1 Pa of argon and for discharge current densities from 25 to 150 A/m<sup>2</sup>. Density fluctuations were recorded, and the maximum rms level was  $< 5.2\%$ . Measured values of  $\tau$  ranged from 0.65 to 0.85  $\mu$ s as the discharge current density was varied over its full range. Assuming the observed turbulent spectrum is composed of ion acoustic waves, we find that  $\tau \propto \langle |\delta E|^2 \rangle^{-0.15}$ , quite different from the prediction. We conclude low-frequency turbulence is not responsible for cross-field electron transport.

## I. INTRODUCTION

Magnetrons are electrical discharge devices used for sputter deposition of thin films.<sup>1,2</sup> Several configurations are in widespread use, including planar, cylindrical, and sputter-gun designs. The common feature of all these designs is the presence of a dc magnetic field  $\mathbf{B}$ , which confines electrons in an  $\mathbf{E} \times \mathbf{B}$  drift loop, thus sustaining the discharge.  $\mathbf{B}$  is low enough, typically 150 G, that only the electrons and not the ions are magnetized. The plasma is exposed to a cathode target where a plasma sheath serves the dual purposes of providing a repulsive electric field for electron confinement and of accelerating ions from the plasma onto the cathode. These ions bombard the cathode and sputter material from it. The population of electrons confined by the plasma sheath at the cathode and the magnetic field above the cathode are quite important to the operation of the magnetron.

Because of this confinement the electron density near the cathode is enhanced and ionization can be sustained at reduced neutral gas pressures. To escape this trap electrons must cross magnetic field lines; therefore, to understand the operation of the magnetron it is necessary to determine the mechanisms responsible for cross-field electron transport.

Spencer and Howson<sup>3</sup> have recently reported that when a planar magnetron is driven to anomalously high current densities negative differential impedance results and that the onset of this phenomenon is correlated with the detection of 15-MHz rf emissions from the plasma. Our experiments were performed at normal operating currents, where we would expect that the high-frequency oscillations reported by Spencer and Howson are not present.

Rossnagel and Kaufman claimed that data from their magnetron experiments agreed with the Bohm diffusion law for cross-field diffusion.<sup>4,5</sup> But, being an empirical scaling law, Bohm diffusion is not a physical model in itself. There are at least three classes of mechanisms which can result in Bohm-like electron transport. One of these is plasma turbulence.<sup>6</sup> Rossnagel and Kaufman speculated that turbulence was responsible for the transport they observed. Previously, low-frequency plasma turbulence was seen in the range of 50 to 500 kHz by Thornton.<sup>7</sup> However, no experiments have

been reported which determine whether there is any correlation between turbulence and electron transport in the magnetron.

Turbulent electric fields  $\delta \mathbf{E}$  result in random  $\delta \mathbf{E} \times \mathbf{B}$  drifts across magnetic field lines.<sup>6</sup> Particles execute a random walk where the displacement is the  $\delta \mathbf{E} \times \mathbf{B}$  drift velocity multiplied by the characteristic time scale of the fluctuating  $\delta \mathbf{E}$  field. This gives rise to a so-called anomalous diffusion coefficient  $D_1$ , that is proportional to the mean-square electric field  $\langle |\delta E|^2 \rangle$ .<sup>8</sup> For cases where plasma transport is dominated by diffusion, the particle confinement time  $\tau$  is proportional to  $D_1^{-1}$ ; therefore, turbulent transport is characterized by the scaling  $\tau \propto \langle |\delta E|^2 \rangle^{-1}$ .

In this paper we report an experiment to test the hypothesis that low-frequency turbulence accounts for cross-field electron transport. We used a dc-biased planar magnetron and a Langmuir probe similar to those used by Rossnagel and Kaufman,<sup>9</sup> as described in Sec. II. Density fluctuations in the same frequency range as reported by Thornton<sup>7</sup> were observed. By characterizing these fluctuations in the time and frequency domains we obtain the rms density fluctuation  $\langle |\delta n/n|^2 \rangle^{1/2}$  as well as  $\langle |\delta E|^2 \rangle$ . We also find  $\tau$  and the scaling of  $\tau$  on  $\langle |\delta E|^2 \rangle$ , which is weak. This forms the basis for our conclusion that low-frequency turbulence is not responsible for electron transport in magnetron plasmas.

## II. APPARATUS

The magnetron used for this experiment is planar, with a cylindrically symmetric magnetic field. The magnetic field is created by a small cylindrical magnet surrounded by a ring of 30 bar magnets (Fig. 1). All magnets are cast Alnico 5. The maximum value of the radial magnetic field, 245 G, occurs at the surface of the cathode at a distance of  $\sim 1.2$  cm from the center. The outer radius of the discharge, determined both from density measurements and the edge of the etch track, is  $\sim 2.5$  cm. The cathode is made of copper and the gas used is argon.

The voltage is provided by a linear power supply operated in the current regulated mode. With neutral pressures of  $\sim 1$  Pa the discharge voltage typically ranges from  $\sim 350$  to

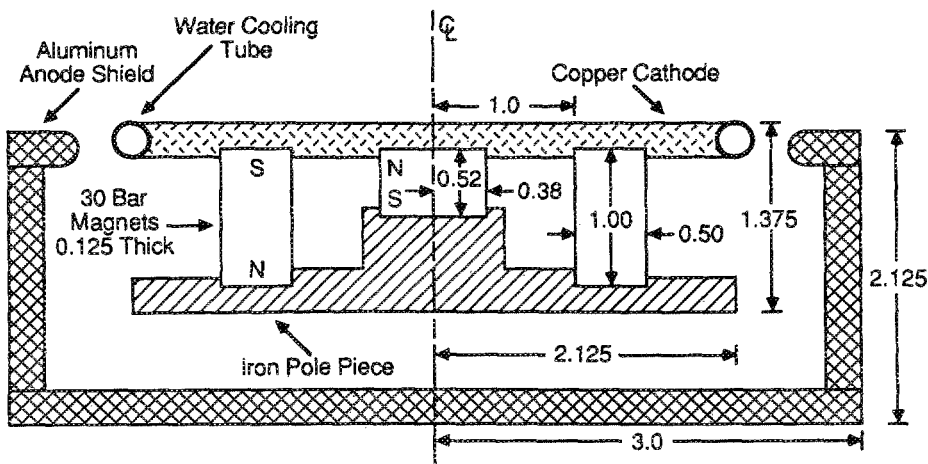


FIG. 1. Schematic drawing of the magnetron. All dimensions are in inches.

— 500 V for discharge currents,  $I_{\text{dis}}$ , of 50 to 300 mA. A switching power supply was also tested, but its voltage ripple (5% at 50 kHz) created density fluctuations, as measured with a Langmuir probe in electron saturation, much larger than those observed using a linear supply. We concluded that use of the switching supply was inappropriate for these turbulence experiments.

Since we want to know the electron confinement time in the magnetron, we need know the size and location of the trapping well. Because of the cylindrical symmetry in the magnetic field (neglecting the spaces between the magnets in the outer ring), the magnetic field can be described solely by the azimuthal component of the magnetic vector potential  $A_\theta(r, z)$ , where  $r$  is radial position,  $\theta$  is azimuthal angle, and  $z$  is axial position. Since neither  $A_\theta$  nor the electrostatic potential  $\phi$  depend on  $\theta$ ,  $\theta$  is an ignorable coordinate. Thus the  $\theta$

component of the canonical momentum  $P_\theta = mr^2\dot{\theta} + qA_\theta r$  is a constant of the motion. Because of this, a charged particle's motion can be described as movement in a two-dimensional effective potential,<sup>10</sup>

$$\psi = \frac{1}{2m} \left( \frac{P_\theta - qrA_\theta}{r} \right)^2 + q\phi,$$

where  $q$  is the particle's charge and  $m$  is the mass. Note that the shape of the effective potential (through the first term) depends on the amount of  $P_\theta$  carried by an individual electron.

To determine the volume of the potential trap we have plotted the first term of the effective potential for  $P_\theta = 0$  in Fig. 2. At  $P_\theta = 0$  the magnetic term of the effective potential gives a very deep well for electrons—over 3500 V for our magnetron. The combination of the magnetic potential with the electrostatic potential of the sheath confines a population of electrons near the surface of the cathode. As was discussed in Sec. I, it is this population of electrons for which we wish to find a confinement time.

The Langmuir probe used is a tungsten wire 0.25 mm in diameter and 3.0 mm long. It is wire wrapped and inserted in an alumina tube with a diameter of 1.6 mm. Only the wire wrap touches the inside of the alumina tube in order to prevent shorting once the probe tip and the alumina tube are sputter coated with copper.<sup>9</sup> The probe is oriented parallel to the surface of the cathode on a ray that intersects the cathode's symmetry axis. It can be moved in both the  $r$  and  $z$  directions, allowing two-dimensional mapping of the plasma.

### III. DATA ACQUISITION AND ANALYSIS

The purpose of the experiment is to determine how  $\tau$  scales with  $\langle |\delta E|^2 \rangle$ ; therefore, we must find values for  $\tau$  and  $\langle |\delta E|^2 \rangle$ . The value of  $\tau$  can be determined indirectly from the number of electrons in the trap and the rate at which they escape, and the value of  $\langle |\delta E|^2 \rangle$  can be computed by recording density fluctuations and assuming a specific dispersion relation for the turbulent waves.

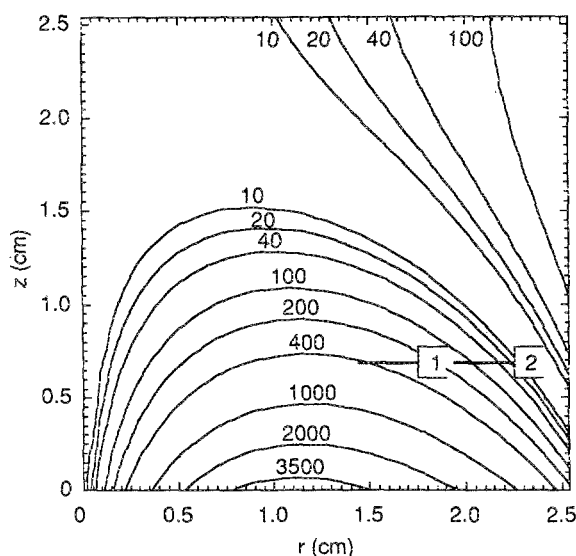


FIG. 2. Contour plot of the calculated effective magnetic potential  $\psi = q^2 A_\theta^2 / (2m)$ , seen by an electron with  $P_\theta = 0$ . Contour values are in volts. The presence of the plasma sheath prevents electrons from escaping to the cathode. Probe positions 1 and 2 are indicated. The surface of the cathode is at  $z = 0$  cm.

The confinement time can be written as<sup>6</sup>

$$\tau = N / \frac{dN}{dt},$$

where  $N$  is the total number of electrons in the trap. The loss rate  $dN/dt$  is given by  $I_{\text{dis}}/e$ , where  $e$  is the electron charge. Finally,  $\tau$  is given by

$$\tau = eN/I_{\text{dis}}. \quad (1)$$

To measure  $N$  we use the Langmuir probe to determine the local density of electrons at a number of different points in the trap. First, the plasma potential  $V_p$  is extracted from the probe characteristic; this is the voltage at which the derivative of dc collected current  $I$ , with respect to the retarding potential, is a maximum.<sup>11</sup> (Collected electron current is taken to be positive.) Data points for  $I < 0.75 I(V_p)$  are then fit to a model for the characteristic that is the sum of a linear term and an exponential term. The electron temperature  $T_e$  is determined from the growth rate of the exponential and the density is found from the values of  $I(V_p)$ ,  $T_e$ , and the probe area. These density measurements are then integrated over the volume of the trap to give  $N$ .

Electric field fluctuations are computed from  $\delta I$ , the fluctuations in  $I$ . We set the probe bias to the plasma potential, which minimizes the perturbation of the plasma, and measure both  $I$  and  $\delta I$ . Since  $I$  is proportional to the plasma density  $n$  and the average electron velocity,  $\delta n/n \approx \delta I/I$  assuming the average electron velocity remains nearly constant. The time history of  $\delta I$  is taken by measuring the voltage across a 46.9- $\Omega$  resistor with an ac coupled 8-bit transient recorder sampling 8192 points with 0.2  $\mu$ s between points. This digitizing rate gives a Nyquist frequency of 2.5 MHz. A 1300-pF capacitor is put in parallel with the resistor to act as a low pass current filter with a bandwidth of 2.6 MHz, thereby preventing aliasing.<sup>12</sup>

The record of the density fluctuations can then be related to  $\delta E$ . Assuming that the electrons are in thermal equilibrium, the electron density must obey

$$n_e(\phi) = n_0 \exp(e\phi/k_b T_e), \quad (2)$$

where  $k_b$  is Boltzmann's constant. Provided that  $\delta n/n \ll 1$ , which we find to be true, an expansion of Eq. (2) tells us that

the potential fluctuations  $\delta\phi$  are related to the density fluctuations by

$$\delta n/n \approx (e/k_b T_e) \delta\phi.$$

The electric field is given by  $\mathbf{E} = -\nabla\phi$ . (This assumes that the modes are electrostatic, which is true at the low frequencies measured.) Considering only one dimension, the Fourier components of  $E$  are related to those of  $\phi$  by

$$\delta E_{kf} = -ik\delta\phi_{kf}, \quad (3)$$

where  $i$  is  $\sqrt{-1}$ ,  $k$  is the wave number, and  $f$  is the frequency. To proceed further we make an assumption about the dispersion relation of the turbulent modes.

Since the electrons are magnetized and experience a dc electric field, they drift at the  $\mathbf{E} \times \mathbf{B}$  velocity through the unmagnetized ions. For typical values of the radial magnetic field and the electric field perpendicular to the cathode measured in the trap region (150 G and 300 V/m), the drift velocity  $v_d$  is  $2 \times 10^4$  m/s. The ion acoustic velocity  $c_s$  is  $3.1 \times 10^3$  m/s for  $T_e = 4$  eV in an argon plasma. When  $v_d > c_s$ , the ion acoustic mode is unstable<sup>10</sup>; therefore, it is reasonable to assume that the turbulent modes are ion acoustic waves. When the ions are unmagnetized, these modes obey the dispersion relation

$$2\pi f = c_s k (1 - f^2/f_{pi}^2)^{1/2},$$

where  $f_{pi}$  is the ion plasma frequency. This reduces to

$$2\pi f = c_s k \quad (4)$$

when  $f \ll f_{pi}$  ( $f_{pi} = 3.3$  MHz at  $n = 10^{16} \text{ m}^{-3}$ ).

When the dispersion relation presented in Eq. (4) is used in Eq. (3) and the resulting expression is squared, we find that

$$|\delta E_f|^2 = \left( \frac{2\pi}{c_s} \right)^2 \left( \frac{k_b T_e}{e} \right)^2 f^2 \left| \frac{\delta n_f}{n} \right|^2. \quad (5)$$

Thus we see that the electric field fluctuation squared is proportional to the frequency squared times the density fluctuation squared. The final step in finding  $\langle |\delta E|^2 \rangle$  from  $|\delta E_f|^2$  uses the fast Fourier transform and the discrete form of Parseval's theorem to perform the averaging operation in the frequency domain.<sup>12</sup>

TABLE I. Plasma parameters as a function of the discharge current at 1.1 Pa, including  $\tau$ ,  $N$ , and parameters measured at positions 1 and 2.

$I_{\text{dis}}$ (A)	$N$ ( $\times 10^{11}$ )	$\tau$ ( $\mu$ s)	Position	$V_p$ (V)	$T_e$ (eV)	$n_e$ ( $\times 10^{16} \text{ m}^{-3}$ )	$\delta n/n$ (%)	$\langle  \delta E ^2 \rangle$ (V/m) <sup>2</sup>
0.0536	2.17	0.648	1	-2.38	4.49	1.49	5.12	7630
			2	-1.09	3.76	0.98	4.04	5660
0.0856	4.12	0.759	1	-1.24	3.77	2.69	3.73	3700
			2	-0.38	3.14	1.94	2.82	2470
0.127	6.52	0.826	1	-0.89	3.55	4.16	2.69	2160
			2	-0.01	2.81	3.26	2.09	1270
0.168	8.77	0.836	1	-0.73	3.40	5.60	2.46	1760
			2	0.03	2.72	4.16	2.04	1120
0.227	12.1	0.856	1	-0.74	3.29	7.69	2.07	1350
			2	0.04	2.59	6.01	1.90	1050
0.303	16.2	0.854	1	-0.70	3.14	10.5	2.13	1170
			2	-0.16	2.54	8.56	1.99	820

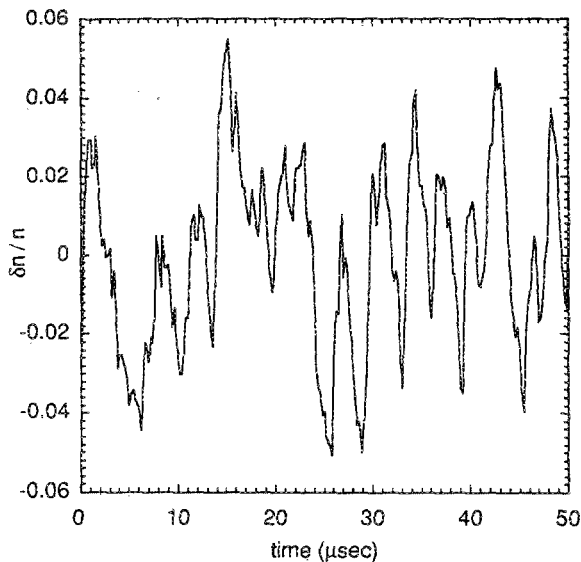


FIG. 3. Time history of density fluctuations taken at position 1 for a discharge current of 0.127 mA. Points were taken every  $0.2 \mu\text{s}$ , and the first 251 points out of 8192 recorded are shown.

#### IV. RESULTS

All data were taken with a neutral pressure of 1.1 Pa of argon. Six runs were done, each with a different value of  $I_{\text{dis}}$ , ranging from 54 to 303 mA. These values of discharge current correspond to current densities of  $\sim 25$  to  $150 \text{ A/m}^2$  averaged over the area of the etch track.

For each run we determined the number of electrons in the trap  $N$  and then computed  $\tau$  using Eq. (1). These values are listed in Table I. To compute  $N$  we measured the electron density at 17 points in the trap ranging over  $r = 0.6$  to  $2.1 \text{ cm}$  and  $z = 0.43$  to  $1.28 \text{ cm}$ , and then integrated over volume. In performing the integral the values of density measured at  $z = 0.43 \text{ cm}$  were assumed to extend back to the surface of

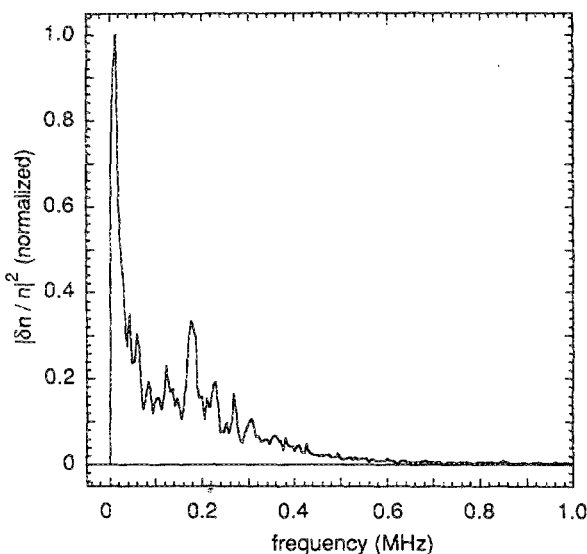


FIG. 4. Spectrum of  $|\delta n/n|^2$ . This spectrum was computed by averaging together 15 overlapping spectra each containing 1024 points.

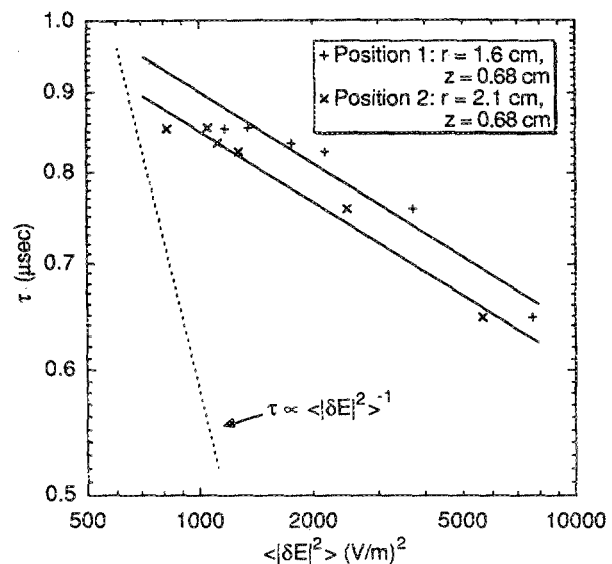


FIG. 5. Scaling of  $\tau$  with  $\langle |\delta E|^2 \rangle$ . Note the log-log axes. The broken line is the prediction of turbulence theory. In both cases the line of best fit has a slope of  $-0.15$ , much less than the value of  $-1$  predicted.

the cathode. We found that  $\tau$  ranged from  $0.65 \mu\text{s}$  at the lowest discharge current to  $0.85 \mu\text{s}$  at the highest, and in fact leveled off at the higher values of  $I_{\text{dis}}$ .

In order to determine  $\langle |\delta E|^2 \rangle$  we recorded  $\delta n/n$  at two positions in the plasma (see Fig. 2). Position 1 is at  $r = 1.6 \text{ cm}$ ,  $z = 0.68 \text{ cm}$  and position 2 is at  $r = 2.1 \text{ cm}$ ,  $z = 0.68 \text{ cm}$ . The magnetic field measured with a Hall probe at position 1 is almost completely radial ( $B_z = 7.6 \text{ G}$  and  $B_r = 132 \text{ G}$ ) and at position 2 is at  $34^\circ$  to the probe ( $B_z = -74 \text{ G}$  and  $B_r = 110 \text{ G}$ ).

Figure 3 shows a short section of the turbulent density fluctuations recorded at position 1 for  $I_{\text{dis}} = 0.127 \text{ A}$ , and Fig. 4 shows the averaged power spectrum for the entire record. The low-frequency peak in the spectrum is close to the argon-ion cyclotron frequency, which is at  $5.0 \text{ kHz}$ . Above  $200 \text{ kHz}$  the spectrum begins to roll off and is comparable to the background noise at  $1 \text{ MHz}$ .

Values for  $\langle |\delta E|^2 \rangle$  were determined using Eq. (5) and integrating the spectrum of  $|\delta E|^2$  up to  $1 \text{ MHz}$ . The integration was cut off at  $1 \text{ MHz}$  for two reasons. First, the signal-to-noise ratio is small above  $1 \text{ MHz}$ . Since Eq. (5) requires that the  $|\delta n/n|^2$  spectrum be weighted by  $f^2$  when  $\langle |\delta E|^2 \rangle$  is computed, a poor signal-to-noise ratio at high frequencies introduces significant errors in  $\langle |\delta E|^2 \rangle$  unless the range of integration is limited. Second, a  $1\text{-MHz}$  integration bandwidth allows us to use the simplified ion acoustic dispersion relation, Eq. (4), which is accurate only for  $f \ll f_{pi}$ . The spike in the  $|\delta n/n|^2$  spectrum at low frequency makes a negligible contribution to  $\langle |\delta E|^2 \rangle$  because of the  $f^2$  weighting.

Values for the rms electric field ( $\langle |\delta E|^2 \rangle^{1/2}$ ) range from  $87 \text{ V/m}$  at the lowest discharge current to only  $29 \text{ V/m}$  at the highest. These values are somewhat less than the perpendicular component of the dc electric field, which, as indicated previously, is of the order of  $300 \text{ V/m}$ . The rms density fluctuations were small,  $< 5.2\%$  (see Table I).

The scaling of  $\tau$  with  $\langle |\delta E|^2 \rangle$  is shown in Fig. 5 for posi-

tions 1 and 2. For both positions the line of best fit (on a log-log plot) has a slope of  $-0.15$ . That is to say,  $\tau \propto \langle |\delta E|^2 \rangle^{-0.15}$ . The fit was determined independently for each position.

## V. CONCLUSIONS

The fact that the confinement times correspond to frequencies greater than 1 MHz gives an indication that the observed turbulence is probably not responsible for electron transport. The random walk diffusion model assumes that the cumulative effect of many collisions (either with particles or waves) moves electrons across magnetic field lines. This assumption of multiple collisions with these low-frequency waves is unlikely to be valid since the measured fluctuation spectrum falls off rapidly above 200 kHz.

Even more convincing is the measured scaling of  $\tau$  with  $\langle |\delta E|^2 \rangle$ . It is not even close to the prediction based on a random walk argument that  $\tau \propto \langle |\delta E|^2 \rangle^{-1}$  for turbulent transport; therefore, we conclude that low-frequency ( $f < f_{pi}$ ) fluctuations are not responsible for cross-field electron transport in the magnetron plasmas.

## ACKNOWLEDGMENTS

This work was supported by the Iowa Department of Economic Development and an IBM Faculty Development Award.

- <sup>1</sup>J. A. Thornton and A. S. Penfold, in *Thin Film Processes*, edited by J. L. Vossen and W. Kern (Academic, New York, 1978), p. 75.
- <sup>2</sup>R. K. Waits, in Ref. 1, p. 131.
- <sup>3</sup>A. G. Spencer and R. P. Howson, *Vacuum* **38**, 497 (1988).
- <sup>4</sup>S. M. Rossmagel and H. R. Kaufman, *J. Vac. Sci. Technol. A* **5**, 88 (1988).
- <sup>5</sup>S. M. Rossmagel and H. R. Kaufman, *J. Vac. Sci. Technol. A* **6**, 223 (1988).
- <sup>6</sup>F. F. Chen, *Introduction to Plasma Physics and Controlled Fusion*, 2nd ed. (Plenum, New York, 1984), p. 190.
- <sup>7</sup>J. A. Thornton, *J. Vac. Sci. Technol.* **15**, 171 (1978).
- <sup>8</sup>A. A. Vedenov, *Theory of Turbulent Plasma* (London Hiffe, New York, 1968), p. 96.
- <sup>9</sup>S. M. Rossmagel and H. R. Kaufman, *J. Vac. Sci. Technol. A* **4**, 1822 (1986).
- <sup>10</sup>G. Schmidt, *Physics of High Temperature Plasmas*, 2nd ed. (Academic, New York, 1979), p. 222.
- <sup>11</sup>T. E. Sheridan and M. A. Hayes, *Rev. Sci. Instrum.* **59**, 1081 (1988).
- <sup>12</sup>W. H. Press, B. P. Flannery, S. A. Teukolsky, and W. T. Vetterling, *Numerical Recipes* (Cambridge University, Cambridge, 1986), Chap. 12.